

1 **Title:** Functional Redundancy in Ocean Microbiomes Controls Trait Stability

2

3 **Authors:** Taylor M. Royalty<sup>1</sup> and Andrew D. Steen<sup>1,2</sup>

4 **Affiliations:** University of Tennessee Departments of Microbiology<sup>1</sup> and Earth and Planetary

5 Sciences<sup>2</sup>

6 **Abstract:**

7 Theory predicts that functional redundancy in microbial communities increases trait stability,  
8 meaning that traits or functions are less likely to be lost from the community when species go  
9 extinct. However, few experiments have empirically tested this prediction, especially in the  
10 context of microbial communities and at the landscape scale. In part, the lack of metrics for  
11 functional redundancy in microbial ecosystems has prevented addressing this question. In a  
12 companion manuscript we proposed a quantitative metric for functional redundancy called  
13 Contribution Evenness (CE) that is optimized to reflect trait stability. Here, we use CE to predict  
14 the stability of marine microbial functions to species and transcription loss. Using transcriptomes  
15 deposited in the Ocean Microbial Reference Gene Catalog (OM-RGC.v2), a catalog of genes and  
16 transcripts sequenced by the TARA Ocean expedition, we quantified the functional redundancy  
17 for 4,314 KEGG Orthologs (KOs) across 124 marine sites. Functional redundancy was highly  
18 correlated with a latent variable consisting of four ocean physiochemical parameters: oxygen and  
19 chlorophyll a concentrations, depth, and salinity. Functional redundancy was higher at the poles  
20 than in non-polar regions. Simultaneously, regional  $\beta$ -diversity for individual functions was  
21 higher for functions with higher functional redundancy. These observations provide evidence  
22 that higher functional redundancy indicates increased stability of microbial ecosystem functions  
23 on spatiotemporal scales consistent with surface ocean mixing. We suggest that future changes in  
24 ocean physiochemistry could likely influence this stability for functions with lower functional  
25 redundancy.

26 **Importance**

27 Functional redundancy describes the state of multiple species performing the same function.  
28 Theory suggests functional redundancy stabilizes microbial community functions from  
29 disturbances leading to species loss or other changes to the microbiome. Previous work suggests  
30 that functional redundancy is common in ocean microbiomes which implies traits should be  
31 more stable among metacommunities. Some laboratory experiments demonstrate this idea, but it  
32 is difficult to test in the natural world. In a companion manuscript, we proposed a functional  
33 redundancy metric sensitive to trait stability. Here, we used this metric to show that functional  
34 redundancy varied substantially among ocean microbiomes and that regions with higher  
35 functional redundancy had higher regional trait stability. Last, we noted that variations in  
36 functional redundancy strongly correlated to ocean physiochemistry. Thus, changes in ocean  
37 physiochemistry via climate change may alter community traits to become more or less resistant  
38 to disturbance relative to contemporary conditions.

## 39 **Introduction**

40           The ability to resolve complete genomes in microbial communities via contig binning and  
41 single-cell genome sequencing has revealed that metabolic functions, or traits, are often present  
42 in multiple taxa within a microbiome (1–4). The practical consequences of functional  
43 redundancy, in terms of community composition and function, are not well understood for  
44 microbial communities. Theoretical predictions, developed in the context of macroecosystems,  
45 suggest that functional redundancy can buffer a community against function loss due to species  
46 extinction (5–9). Foundational work on grassland ecosystems validated these theoretical  
47 predictions by showing that plant community biomass stability increased with higher functional  
48 redundancy (10). Mesocosm experiments provide empirical evidence that functional redundancy  
49 may also buffer microbial ecosystem functions from species loss. For instance, microbial density  
50 and biomass was less variable for assemblages with redundant populations occupying different  
51 trophic guilds in a food web (11), and reduction-oxidation conditions in sediment communities  
52 were more stable with higher bacterial diversity and niche overlap (12). Although existing  
53 theoretical and empirical evidence suggests functional redundancy may enhance ecosystem  
54 function stability, small-scale and mesocosm experiments with microbial communities may not  
55 reflect the most important processes on ecosystem scales (13). Establishing whether functional  
56 redundancy stabilizes traits is important for understanding how environmental fluctuations, most  
57 notably climate change, may influence microbially-mediated biogeochemical cycles.

58           In a companion paper, we developed a metric for functional redundancy called  
59 contribution evenness (CE) (14). CE uses genes or transcripts as traits (15, 16) and measures  
60 how evenly taxa contribute to the community-wide level of these traits (total gene abundance in  
61 the case of genes, and total transcript abundance in the case of transcripts). CE is optimized to

62 reflect how stable microbially-catalyzed functions are to random species extinction or  
63 transcription loss in communities. Here, we use CE to address three fundamental questions about  
64 functional redundancy in marine microbial metacommunities:

- 65 1.) Does functional redundancy of ocean microbiomes vary geographically,
- 66 2.) If so, does this variation relate to the physicochemical environment, and
- 67 3.) What ecological consequences are apparent from observed patterns in functional redundancy?

68 To answer these questions, we used KEGG orthology (KO) annotations of genes reported  
69 from 180 sites sampled during the TARA Oceans expeditions, plus transcripts reported from a  
70 subset of 124 of those sites (17). KEGG is an attractive ontology because the functions of KOs  
71 are biochemically well-characterized and provide a reasonably large coverage of predicted genes  
72 in marine microbiomes. The *TARA Oceans* dataset is ideal for this work because it encompasses  
73 a diverse set of sites and marine ecosystems, which were sampled with generally standardized  
74 methods (18). By applying CE to the *TARA Oceans* data set, we identified geographic variations  
75 in functional redundancy, identified physicochemical factors relating to this variation, and  
76 established that microbial functions were less stable in regions with lower functional  
77 redundancy. These observations combined allowed us to identify some possible effects that  
78 climate change may have on the resilience of microbial community function to local disturbance.

## 79 **Methods**

### 80 *TARA Oceans Genes and Environmental Data*

81 We downloaded the entire Ocean Microbial Reference Gene Catalog v2 (OM-GRC.v2)  
82 on 1 Feb 2021 from EMBL-EBI (BioStudy: S-BSST297) and the environmental data from  
83 <https://doi.org/10.5281/zenodo.3473199> (17). This data set includes annotations and abundance

84 for metagenomes from 180 unique sites and transcriptomes from 124 sites. Gene and transcript  
85 profiles correspond to biological sequences collected from 100L of seawater on filters with size  
86 ranges 0.22-1.6  $\mu\text{m}$  or 0.22-3.0  $\mu\text{m}$  (18). Analysis was limited to sequences in OM-RGC.v2  
87 annotated to KEGG orthologs (KO) (19). We interpreted length-normalized short-read mapping  
88 frequencies as abundances. These values reflect the abundance of any sequence in a  
89 metagenome or transcriptome, given a fixed sequencing effort. Gene abundances for KO single  
90 copy marker genes (list below) annotated to the same genus were averaged to estimate the  
91 abundance of a given genus. Our selection of genus level analysis was to mitigate noise  
92 associated with analyzing functional redundancy of ASVs, which is theoretically possible. To  
93 allow for meaningful comparisons of functional redundancy at different sites, we rarified  
94 sequencing effort at each site. Relative abundances were then used as weights during random  
95 sampling, with replacement. Each site was sampled 3358334 and 472163 times for gene and  
96 transcript profiles, respectively. These values corresponded to the lowest sampling effort among  
97 all metagenomes and transcriptomes, respectively.

#### 98 *KO Functional Redundancy and Diversity*

99 Functional redundancy was calculated for each KO at each site for both metagenomes  
100 and metatranscriptomes. Functional redundancy was calculated with Contribution Evenness (CE)  
101 as detailed in the companion paper (14). Here, we treat KOs as proxies for metabolic traits (16,  
102 20). In brief, the abundance of sequences sharing the same KO annotation in a sample was  
103 summed together, without regard to genus. Subsequently, the abundance of genes for individual  
104 genera was normalized by the summed abundance to obtain a relative abundance of each gene,  
105 for each genus. This vector corresponds to the relative contribution distribution (equation 3.2 in  
106 the companion paper). Species richness ( $S$ ) used for calculating CE in equation 8 in companion

107 paper was calculated with KO single copy marker genes. The presence of a genus was  
108 determined by summing the abundance of single copy marker genes: K06942, K01889, K01887,  
109 K01875, K01883, K01869, K01873, K01409, K03106, and K03110. If the summed abundance  
110 was greater than 0, then the genus was considered present in the metagenome/metatranscriptome.

### 111 *Global Modeling of Functional Redundancy*

112 We sought to characterize spatial trends in the functional structure of microbial  
113 communities. To do this, we performed redundancy analysis using the rda function from the R  
114 package, *vegan* (21). In this analysis, the functional structure of microbial communities was  
115 treated as a response variable and physio-chemical variables were treated as predictor variables.  
116 For sites where a given KO was absent, the KO was assigned a value of zero. This situation  
117 occurred ~13.6% and 18.5% of the time for gene and transcript profiles, respectively. Low  
118 functional redundancy does not necessarily imply that a function is ecologically unimportant.  
119 This is particularly true for traits with low functional redundancy that strongly correlate to  
120 phylogeny. Such examples include *Thaumarchaeota* and diazotrophs which act as the primary  
121 nitrifiers and nitrogen fixers in the ocean, respectively (22). On the contrary, small changes in  
122 functional redundancy for traits with low functional redundancy might reflect key ecological  
123 processes, and thus, comparisons of community functional structure should account for the  
124 differences in functional redundancy magnitude. Thus, changes in KO functional redundancy  
125 reflected changes with respect to the KO's observed variance while not reflecting the KO's order  
126 of magnitude, which spanned five orders of magnitude. To prevent functions with large CE from  
127 dominating the redundancy analysis, we normalized CE for each KO at each site by the  
128 respective KO's variance from across all sites. For the redundancy analysis, we used salinity  
129 (PSU), nitrate ( $\text{mmol m}^{-3}$ ), phosphate ( $\text{mmol m}^{-3}$ ), oxygen ( $\text{mmol m}^{-3}$ ), chlorophyll A ( $\text{mg m}^{-3}$ ),

130 depth (m), and silicate ( $\text{mmol m}^{-3}$ ). We chose these variables as they were *in situ* measurements  
131 (18) and could scale with models that predict global ocean chemistry. We imputed missing data,  
132 as removing incomplete cases can bias datasets (23). Random forest imputation was performed  
133 using the `missForest` function, from the R package, `missForest` (24). Next, each environmental  
134 variable was converted into a normal distribution using a boxcox transformation via the `boxcox`  
135 function in the R package, `MASS` (25). Variables were then centered to have a mean of zero.  
136 Last, the significance of each variable as well as the first two canonical axes was verified using  
137 the `anova.cca` function in the R Package, `vegan` (21).

138         The first canonical axis derived from the redundancy analysis was used to predict mean  
139 transcript functional redundancy from the individual metatranscriptomes (sites) using OLS  
140 regression. This model was compared to an OLS regression using salinity, nitrate, phosphate,  
141 oxygen, chlorophyll A, depth, and silicate as predictors of mean transcript functional  
142 redundancy. Similar to before, missing data were imputed using `missForest` (24), variables were  
143 transformed with a boxcox transformation (25), and variables centered so the mean distribution  
144 was zero prior to regression. The best predictor subset was determined using the `regsubsets`  
145 function from the R package, `leaps` (26). The criteria defining the best model was minimizing  
146 AIC.

147         The monthly-averaged data products spanning from Jan 2013 to Dec 2018 for  
148 `GLOBAL_REANALYSIS_BIO_001_029` and `GLOBAL_REANALYSIS_PHY_001_031` were  
149 downloaded from <https://marine.copernicus.eu/> on 7 May 2021. Data products had a grid  
150 resolution of  $0.25^\circ \times 0.25^\circ$ . The OLS regression using the first canonical axis as a predictor  
151 substantially outperformed the best subset OLS when predicting mean transcript functional  
152 redundancy. We therefore converted the predicted data product chemistry for each grid cell into

153 a score for the first canonical axis. Then, the mean transcript functional redundancy was  
154 predicted for each grid cell, for each month, utilizing the coefficient derived from the canonical  
155 axis OLS regression. The median, 5<sup>th</sup> percentile, and 95<sup>th</sup> percentile of mean functional  
156 redundancy was taken across the six-year window. Variance was measured as the difference  
157 between the 95<sup>th</sup> and 5<sup>th</sup> percentile divided by the median.

### 158 *Metatranscriptome $\beta$ -diversity and Trait Stability*

159 The  $\beta$ -diversity (27) was calculated for individual functions (KO) across different  
160 regions. Regions were defined as a metatranscriptome and the nine closest metatranscriptomes in  
161 the epipelagic (depth < 200m). Site distances were measured using the published site coordinates  
162 (17) and the *distm* (default parameters) function from the R package, *geosphere* (28). Redundant  
163 combinations of sites were removed prior to reporting results. The average functional  
164 redundancy for individual functions was taken for each region. The  $\beta$ -diversity was calculated as:

$$165 \quad D(H_{\beta}) = \frac{D(H_{\gamma})}{D(H_{\alpha})} \quad (2)$$

166 Here, we used a diversity order  $q=0$ , or the richness to calculate diversity. As such,  $\gamma$ -diversity  
167 was either 0 (regionally absent) or 1 (regionally present), and  $\alpha$ -diversity was the proportion of  
168 local communities with the trait. Since  $\beta$ -diversity is not defined for traits completely absent  
169 from a region, the  $\beta$ -diversity calculation simplified to:

$$170 \quad D(H_{\beta}) = \frac{1}{f} \quad (3)$$

171 which is simply the inverse proportion ( $f$ ) of local communities in a region with a given function.

## 172 **Results and Discussion**

173 We used CE (14) to measure functional redundancy for KEGG ortholog (KO)-annotated  
174 genes from 180 and 124 *TARA Oceans* metagenomes and metatranscriptomes, respectively (17).  
175 CE uses genes (CE with respect to genes) or transcripts (CE respect to transcripts) as traits (15,  
176 16) and measures how evenly species in a community contribute to these traits as a whole. After  
177 calculating CE for metagenomes (Fig. 1A) and metatranscriptomes (Fig. 1B), we found that KOs  
178 spanned over three orders of magnitude, demonstrating the high degree of variability in how  
179 functionally redundant traits are in the ocean. We further isolated KOs based on KEGG energy  
180 metabolism classification to illustrate how functional redundancy varied across the ocean for  
181 sulfur, photosynthesis, oxidative phosphorylation, nitrogen, methane, and carbon fixation. The  
182 distribution of transcript abundance within ocean microbiomes correlated well with the  
183 distribution of gene abundance at the same site (Fig. 1C;  $R^2=0.45$ ,  $p<0.001$ ). This relationship  
184 was not surprising considering previous reports that metagenome gene abundances strongly  
185 influenced transcript abundances across *TARA Oceans* microbiomes (17). Although the nature of  
186 these observations is similar, the ecological implication is different. Specifically, the observation  
187 of Salazar et al. shows correlation in absolute gene abundance and transcription abundance,  
188 whereas our observation indicates that when genomic traits are more evenly distributed across  
189 genus within a community, transcription is also more evenly distributed across genus.

190 To better understand the relationship between environmental characteristics and  
191 functional redundancy, we used redundancy analysis (RDA) to model the functional redundancy  
192 of each KO at each site as a function of the seven environmental parameters: salinity, depth, and  
193 concentrations of nitrate, phosphate, and silicate ions, oxygen, and chlorophyll a (Fig. 1). The  
194 first canonical axis of this model explained 19.8% of the total functional redundancy variance in  
195 4,314 transcripts annotated as KOs. An ANOVA demonstrated that the first canonical axis

196 explained significantly more variability in KO functional redundancy than a null model ( $p < 0.01$ )  
197 (29). Although the total explanatory power for individual KOs was low, we found that the  
198 average functional redundancy of all KOs at each TARA Oceans site was accurately predicted by  
199 the first canonical axis alone (93.2% of total variance explained; ordinary least squares  
200 regression).

201       Factor loadings of this first canonical axis were dominated positively by oxygen and  
202 chlorophyll a and negatively by sample depth and salinity (Fig. 2B). Thus, this canonical axis  
203 appears to be a proxy for phototroph biomass, or the extent to which an environment is  
204 dominated by copiotrophs versus oligotrophs. The strong predictive power of chlorophyll a was  
205 not surprising given that carbon export mediated by primary productivity is known to be a good  
206 predictor for community composition and genomic composition in the ocean (30). Higher  
207 functional redundancy was positively correlated with this proxy for phototroph biomass. We  
208 compared the performance of our factor-based model to a best subset (based on an AIC criteria)  
209 OLS regression using the original seven physiochemical variables ( $\text{NO}_3^-$ ,  $\text{PO}_4^{3-}$ , salinity, depth,  
210  $\text{O}_2$ , Si, and ChlA) that generated our factor (Fig. 2C). In contrast to the factor model, the best  
211 subset model ( $\text{O}_2$ , Si, and depth) explained only 32.4% of the variance in mean functional  
212 redundancy.

213       The high explanatory power by the environmental data justified extrapolating our factor  
214 model onto a global scale. Using global predictions of ocean nutrient concentrations, we  
215 calculated factor scores at a  $0.25^\circ \times 0.25^\circ$  resolution and predicted functional redundancy across  
216 Earth's oceans using the derived coefficient from our OLS regression of mean functional  
217 redundancy versus the first canonical axis of the RDA. Our model predicts that functional  
218 redundancy is highest in polar regions and near river outflows, and lowest in subtropical gyres

219 (Fig. 3A). Variance was highest in polar regions, coastal regions, and river outflows (Fig. 3B).  
220 The transition from high to low functional redundancy between polar and non-polar latitudes was  
221 consistent with previously reported ecological boundaries for ocean microbiomes, where the  
222 transition from non-polar to polar latitudes corresponded to compositional changes in  
223 metatranscriptomes and metagenomes (17).

#### 224 *Functional Redundancy as an Indicator of Trait Stability*

225 In the companion paper, we presented a numerical simulation demonstrating a  
226 relationship between CE and trait stability to random extinctions. Here, we sought to establish  
227 whether there is empirical evidence that functional redundancy increases trait stability in ocean  
228 microbiomes, as previously hypothesized (31). Specifically, we hypothesized that if higher levels  
229 of functional redundancy do indeed increase trait stability, then the sets of functions present in  
230 nearby communities should be more similar when functional redundancy is higher. To test this  
231 hypothesis, we compared functional redundancy at each epipelagic site to the  $\beta$ -diversity (27) of  
232 each function (coded as present or absent) in a local region consisting of the site in question plus  
233 the nine nearest sites. In this context, lower  $\beta$ -diversity indicates that a larger portion of local  
234 communities shared a given function (equation 3). Since microbial communities exhibit spatial  
235 autocorrelation (32), these ad-hoc local regions serve as a reasonable alternative to the ideal data  
236 set, which would consist of subsequent metagenomes taken from a parcel of water over time.

237 We observed a negative monotonic relationship between functional redundancy and beta  
238 diversity for every KO for every unique region (Fig. 4). This qualitative evidence is consistent  
239 with the idea that functional redundancy maintains trait stability on a regional level. Notably,  
240  $CE > 0.01$  corresponded to functions becoming almost entirely stable within their respective  
241 regions (Fig. 4). This threshold suggests a large portion of functions should be stable across

242 Earth's ocean microbiome (Fig. 3). Nonetheless, select functions do appear vulnerable to  
243 regional instability. Notably, nitrogen metabolism functions tend to have  $CE < 0.01$  (Fig. 1B).  
244 Climate models and historical observations indicate that major ocean currents are slowing (33),  
245 oxygen minimum zones are expanding (34), and there will be future changes in regional primary  
246 productivity (35). With respect to oxygen and primary productivity, these variables are important  
247 in our factor model and suggest that future changes in these parameters might disproportionately  
248 influence the stability for lower functional redundancy functions such as nitrogen energy  
249 metabolism.  
250

251 **Acknowledgements:**

252 Funding for this project was provided by the Department of Energy, Office of Science, Office of  
253 Biological and Environmental Research (DE-SC0020369) to A.D.S.

254 **Competing Interests:**

255 We have no competing interests.

256 **Data and Materials Availability:**

257 The Ocean Microbial Reference Gene Catalog v2 (OM-GRC.v2) is accessible from EMBL-EBI  
258 (BioStudy: S-BSST297). *TARA Oceans* site metadata was downloaded from

259 <https://doi.org/10.5281/zenodo.3473199>. The hindcast data products,

260 GLOBAL\_REANALYSIS\_BIO\_001\_029 and GLOBAL\_REANALYSIS\_PHY\_001\_031, are

261 accessible from <https://marine.copernicus.eu/>. All code and processed data is available at

262 [https://github.com/taylorroyalty/tara\\_ocean\\_fr](https://github.com/taylorroyalty/tara_ocean_fr).

263

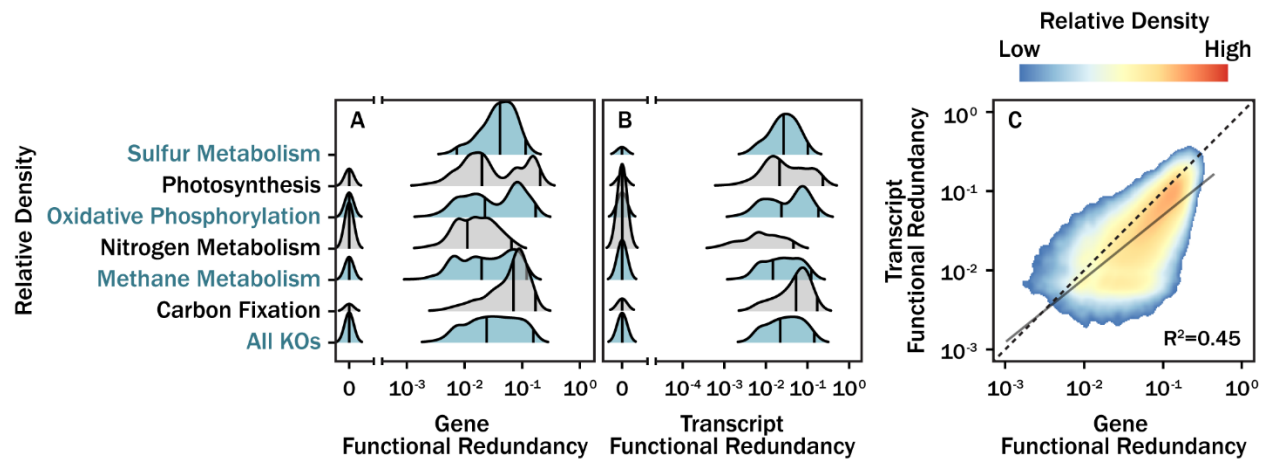
264 **References and Notes:**

- 265 1. Louca S, Polz MF, Mazel F, Albright MBN, Huber JA, O'Connor MI, Ackermann M, Hahn AS,  
266 Srivastava DS, Crowe SA, Doebeli M, Parfrey LW. 2018. Function and functional redundancy in  
267 microbial systems. *Nat Ecol Evol* 2:936–943.
- 268 2. Royalty TM, Steen AD. 2019. Quantitatively Partitioning Microbial Genomic Traits among  
269 Taxonomic Ranks across the Microbial Tree of Life. *mSphere* 4.
- 270 3. Martiny JBH, Jones SE, Lennon JT, Martiny AC. 2015. Microbiomes in light of traits: A  
271 phylogenetic perspective. *Science* (80- ) 350:aac9323.
- 272 4. Delmont TO, Quince C, Shaiber A, Esen ÖC, Lee STM, Rappé MS, McLellan SL, Lückner S, Eren  
273 AM. 2018. Nitrogen-fixing populations of Planctomycetes and Proteobacteria are abundant in  
274 surface ocean metagenomes. *Nat Microbiol* 3:804–813.
- 275 5. Naeem S. 1998. Species Redundancy and Ecosystem Reliability. *Conserv Biol* 12:39–45.
- 276 6. Rosenfeld JS. 2002. Functional redundancy in ecology and conservation. *Oikos* 98:156–162.
- 277 7. Fonseca CR, Ganade G. 2001. Species functional redundancy, random extinctions and the stability  
278 of ecosystems. *J Ecol* 118–125.
- 279 8. Walker BH. 1992. Biodiversity and Ecological Redundancy. *Conserv Biol* 6:18–23.
- 280 9. Cottingham KL, Brown BL, Lennon JT. 2001. Biodiversity may regulate the temporal variability  
281 of ecological systems. *Ecol Lett* 4:72–85.
- 282 10. Tilman D, Reich PB, Knops JMH. 2006. Biodiversity and ecosystem stability in a decade-long  
283 grassland experiment. *Nature* 441:629–632.
- 284 11. Naeem S, Li S. 1997. Biodiversity enhances ecosystem reliability 390:507–509.
- 285 12. Hunting ER, Vijver MG, van der Geest HG, Mulder C, Kraak MHS, Breure AM, Admiraal W.  
286 2015. Resource niche overlap promotes stability of bacterial community metabolism in  
287 experimental microcosms. *Front Microbiol* 6:1–7.
- 288 13. ZoBell CE, Anderson DQ. 1936. Observations on the multiplication of bacteria in different  
289 volumes of stored sea water and the influence of oxygen tension and solid surfaces. *Biol Bull*  
290 71:324–342.
- 291 14. Royalty TM, Steen AD. 2021. Contribution Evenness: A functional redundancy metric for  
292 microbially-mediated biogeochemical rates and processes. *bioRxiv* 6.

- 293 15. Violle C, Navas M-L, Vile D, Kazakou E, Fortunel C, Hummel I, Garnier E. 2007. Let the concept  
294 of trait be functional! *Oikos* 116:882–892.
- 295 16. Green JL, Bohannan BJM, Whitaker RJ. 2008. Microbial biogeography: from taxonomy to traits.  
296 *Science* (80- ) 320:1039–1043.
- 297 17. Salazar G, Paoli L, Alberti A, Huerta-Cepas J, Ruscheweyh HJ, Cuenca M, Field CM, Coelho LP,  
298 Cruaud C, Engelen S, Gregory AC, Labadie K, Marec C, Pelletier E, Royo-Llloch M, Roux S,  
299 Sánchez P, Uehara H, Zayed AA, Zeller G, Carmichael M, Dimier C, Ferland J, Kandels S,  
300 Picheral M, Pisarev S, Poulain J, Acinas SG, Babin M, Bork P, Boss E, Bowler C, Cochrane G, de  
301 Vargas C, Follows M, Gorsky G, Grimsley N, Guidi L, Hingamp P, Iudicone D, Jaillon O,  
302 Kandels-Lewis S, Karp-Boss L, Karsenti E, Not F, Ogata H, Pesant S, Poulton N, Raes J, Sardet  
303 C, Speich S, Stemann L, Sullivan MB, Sunagawa S, Wincker P. 2019. Gene Expression Changes  
304 and Community Turnover Differentially Shape the Global Ocean Metatranscriptome. *Cell*  
305 179:1068-1083.e21.
- 306 18. Pesant S, Not F, Picheral M, Kandels-Lewis S, Le Bescot N, Gorsky G, Iudicone D, Karsenti E,  
307 Speich S, Trouble R, Dimier C, Searson S. 2015. Open science resources for the discovery and  
308 analysis of Tara Oceans data. *Sci Data* 2:1–16.
- 309 19. Kanehisa M, Furumichi M, Tanabe M, Sato Y, Morishima K. 2017. KEGG: New perspectives on  
310 genomes, pathways, diseases and drugs. *Nucleic Acids Res* 45:D353–D361.
- 311 20. Krause S, Le Roux X, Niklaus PA, Van Bodegom PM, Lennon JT, Bertilsson S, Grossart H-P,  
312 Philippot L, Bodelier PLE. 2014. Trait-based approaches for understanding microbial biodiversity  
313 and ecosystem functioning. *Front Microbiol* 0:251.
- 314 21. Philip D. 2003. Computer program review VEGAN , a package of R functions for community  
315 ecology. *J Veg Sci* 14:927–930.
- 316 22. Pajares S, Ramos R. 2019. Processes and Microorganisms Involved in the Marine Nitrogen Cycle:  
317 Knowledge and Gaps. *Front Mar Sci* 0:739.
- 318 23. McElreath R. 2020. *Statistical Rethinking: A Bayesian Course with Examples in R and Stan*, 2nd  
319 ed. CRC Press.
- 320 24. Stekhoven DJ, Bühlmann P. 2012. Missforest-Non-parametric missing value imputation for  
321 mixed-type data. *Bioinformatics* 28:112–118.
- 322 25. Venables WN, Ripley BD. 2002. *Modern Applied Statistics with S*. 7.3.49. Springer, New York.
- 323 26. Lumley T. 2004. *The leaps Package*. 2.7.

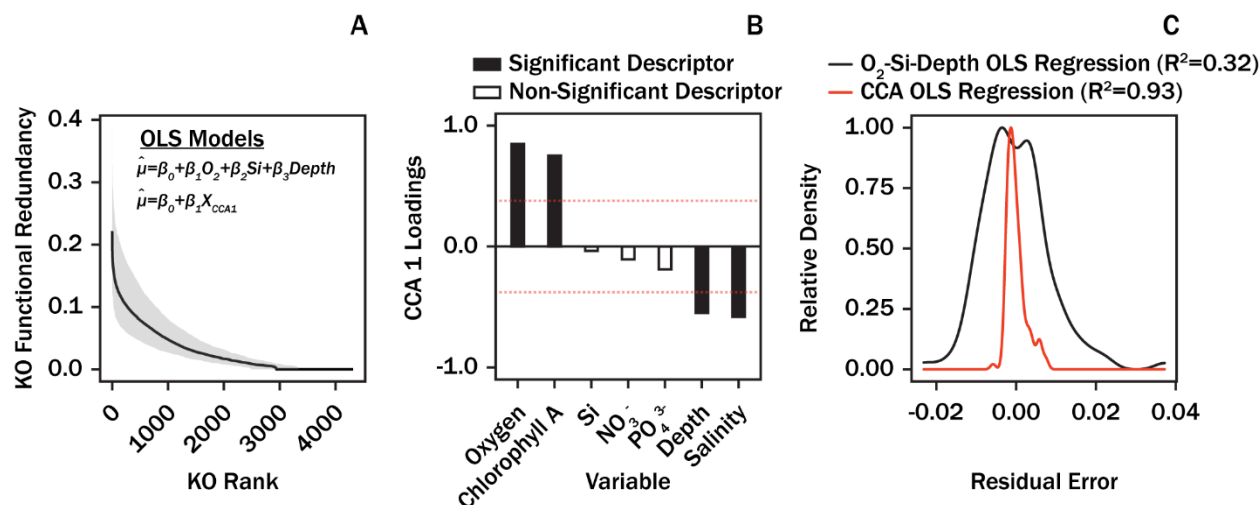
- 324 27. Jost L. 2007. Partitioning diversity into independent alpha and beta components. *Ecology*  
325 88:2427–2439.
- 326 28. Hijmans R, Williams E, Vennes C. 2015. Geosphere: spherical trigonometry. R package. 1.5.
- 327 29. Legendre P, Oksanen J, ter Braak CJF. 2011. Testing the significance of canonical axes in  
328 redundancy analysis. *Methods Ecol Evol* 2:269–277.
- 329 30. Guidi L, Chaffron S, Bittner L, Eveillard D, Larhlimi A, Roux S, Darzi Y, Audic S, Berline L,  
330 Brum JR, Coelho LP, Espinoza JCI, Malviya S, Sunagawa S, Dimier C, Kandels-Lewis S, Picheral  
331 M, Poulain J, Searson S, Stemmann L, Not F, Hingamp P, Speich S, Follows M, Karp-Boss L,  
332 Boss E, Ogata H, Pesant S, Weissenbach J, Wincker P, Acinas SG, Bork P, De Vargas C, Iudicone  
333 D, Sullivan MB, Raes J, Karsenti E, Bowler C, Gorsky G. 2016. Plankton networks driving carbon  
334 export in the oligotrophic ocean. *Nature* 532:465–470.
- 335 31. Lennon JT, Jones SE. 2011. Microbial seed banks: The ecological and evolutionary implications  
336 of dormancy. *Nat Rev Microbiol* 9:119–130.
- 337 32. Ghiglione J-F, Galand PE, Pommier T, Pedrós-Alió C, Maas EW, Bakker K, Bertilson S,  
338 Kirchmanj DL, Lovejoy C, Yager PL, Murray AE. 2012. Pole-to-pole biogeography of surface  
339 and deep marine bacterial communities. *Proc Natl Acad Sci U S A* 109:17633–8.
- 340 33. Caesar L, McCarthy GD, Thornalley DJR, Cahill N, Rahmstorf S. 2021. Current Atlantic  
341 Meridional Overturning Circulation weakest in last millennium. *Nat Geosci* 14:118–120.
- 342 34. Ito T, Minobe S, Long MC, Deutsch C. 2017. Upper ocean O<sub>2</sub> trends: 1958–2015. *Geophys Res*  
343 *Lett* 44:4214–4223.
- 344 35. Fu W, Randerson JT, Keith Moore J. 2016. Climate change impacts on net primary production  
345 (NPP) and export production (EP) regulated by increasing stratification and phytoplankton  
346 community structure in the CMIP5 models. *Biogeosciences* 13:5151–5170.
- 347 36. Legendre P, Legendre L. 2012. *Numerical Ecology*, 3rd ed. Elsevier.
- 348
- 349
- 350

351 **Figures:**



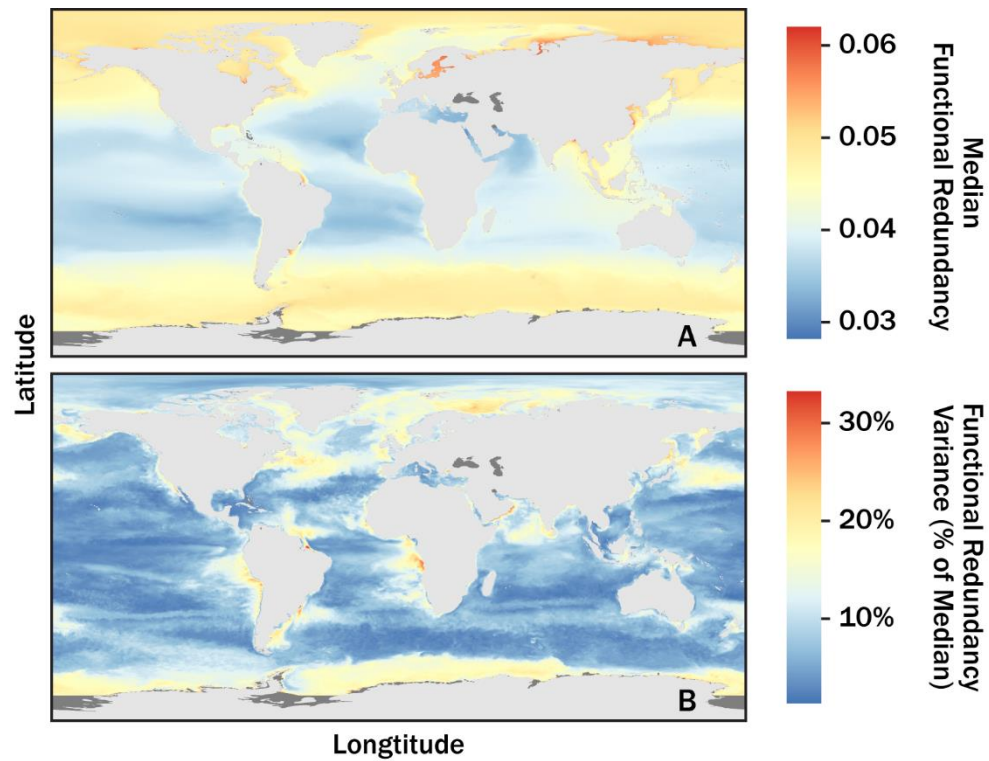
352

353 **Fig. 1:** Variation in functional redundancy for KOs across 180 *TARA Oceans* metagenomes (A),  
354 129 *TARA Oceans* transcriptomes (B), and a pairwise comparison of functional redundancy  
355 ( $n \approx 415,000$ ) for KOs annotated the same at the same site (C). Density curves  
356 (A,B) were generated with a kernel density estimate (gaussian kernel with a bandwidth 0.0803).  
357 The vertical black lines correspond to 5<sup>th</sup>, 50<sup>th</sup>, and 95<sup>th</sup> quantiles. The metagenomes and  
358 metatranscriptomes functional redundancy regression (C) followed a log<sub>10</sub>-log<sub>10</sub> model (solid  
359 black line). Prior to regression, all values were offset by 10<sup>-4</sup> and high leverage data was  
360 removed based on high Cook's distance ( $> \frac{4}{n}$ ). The color gradient and black dashed line  
361 correspond to data density and a one-to-one relationship, respectively.



362

363 **Fig. 2:** Metatranscriptome rank-functional redundancy curves across all *TARA Oceans* sites  
 364 (n=129) analyzed in this study (A). The black line corresponds to the median while the shaded  
 365 area corresponds to the range spanning between the 5<sup>th</sup> and 95<sup>th</sup> percentiles. Proposed models  
 366 were evaluated for accuracy in predicting mean ( $\mu$ ) and standard deviation ( $\sigma$ ) of individual rank-  
 367 functional redundancy curves. The O<sub>2</sub>-Si-Depth model was selected as a best subset (minimum  
 368 AIC) among the seven predictor variables. Canonical axis 1 loadings (scaling = 0) derived from  
 369 the redundancy analysis (B). Dashed red lines in panel (B) correspond to the “equilibrium line of  
 370 descriptors” ( $\sqrt{d/p} = \sqrt{1/7}$ ), a threshold for defining significant variable contribution to factor  
 371 loadings (36). A comparison in residual error of mean functional redundancy predicted by the  
 372 O<sub>2</sub>-Si-Depth OLS regression model and the canonical axis OLS regression model (C).



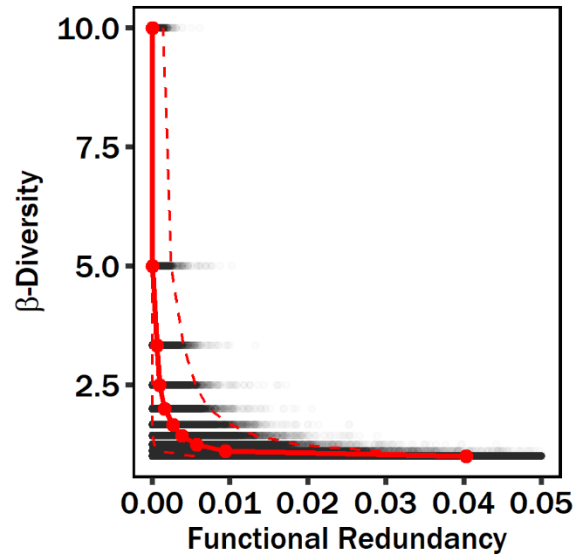
373

374 **Fig. 3:** Mean functional redundancy of all KOs at a 5m depth across Earth's oceans ( $0.25^\circ \times$

375  $0.25^\circ$  resolution). Panels (A) and (B) correspond to the median and variance of predictions

376 spanning Jan 2013 to Dec 2018, respectively. Dark and light grey correspond to regions absent

377 of predictor data and land, respectively.



378 **Fig. 4.** The  $\beta$ -diversity for individual KOs as a function of the average functional redundancy  
379 within local regions. The local region of each site was defined as the site plus the 9  
380 geographically nearest sites. For all regions, the median distance from the region center to sites  
381 within the region is 1740 km. The red points and solid red line correspond to the median  
382 functional redundancy across all KOs for a given  $\beta$ -diversity. The upper and lower dashed red  
383 lines correspond to the 97.5 and 2.5 quantiles, respectively.